

Crystal structure of UDP-*N*-acetylmuramoyl-L-alanine:D-glutamate ligase from *Escherichia coli*

Jay A. Bertrand, Geneviève Auger¹,
Eric Fanchon, Lydie Martin, Didier Blanot¹,
Jean van Heijenoort¹ and Otto Dideberg²

Institut de Biologie Structurale Jean-Pierre Ebel (CEA-CNRS),
Laboratoire de Cristallographie Macromoléculaire, 41 avenue des
Martyrs, F-38027 Grenoble Cedex 1 and ¹Unité de Recherche
Associée 1131 du Centre National de la Recherche Scientifique,
Biochimie Moléculaire et Cellulaire, Université de Paris-Sud, Orsay,
France

²Corresponding author

UDP-*N*-acetylmuramoyl-L-alanine:D-glutamate ligase (MurD) is a cytoplasmic enzyme involved in the biosynthesis of peptidoglycan which catalyzes the addition of D-glutamate to the nucleotide precursor UDP-*N*-acetylmuramoyl-L-alanine (UMA). The crystal structure of MurD in the presence of its substrate UMA has been solved to 1.9 Å resolution. Phase information was obtained from multiple anomalous dispersion using the K-shell edge of selenium in combination with multiple isomorphous replacement. The structure comprises three domains of topology each reminiscent of nucleotide-binding folds: the N- and C-terminal domains are consistent with the dinucleotide-binding fold called the Rossmann fold, and the central domain with the mononucleotide-binding fold also observed in the GTPase family. The structure reveals the binding site of the substrate UMA, and comparison with known NTP complexes allows the identification of residues interacting with ATP. The study describes the first structure of the UDP-*N*-acetylmuramoyl-peptide ligase family.

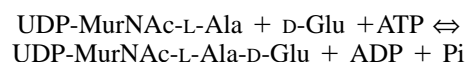
Keywords: drug design/MurD/peptidoglycan/synthetase/
X-ray structure

Introduction

Peptidoglycan or murein is the polymeric mesh of the bacterial cell wall which plays a critical role in protecting the bacteria against osmotic lysis. As a result, the biosynthetic pathway of the UDP-*N*-acetylmuramoyl-pentapeptide, the cytoplasmic peptidoglycan precursor, represents an attractive target for the development of new antibacterial agents. Structural studies of enzymes involved in the pathway have already provided strategies for the rational design of novel inhibitors. To date, the crystal structures of four enzymes of the pathway are known at the atomic level, UDP-*N*-acetylglucosamine enolpyruvyl transferase (MurA) from *Enterobacter cloacae* (Schönbrunn *et al.*, 1996) and *Escherichia coli* (Skarzynski *et al.*, 1996), UDP-*N*-acetylpyruvyl-glucosamine reductase (MurB) from *E. coli* (Benson *et al.*, 1995)

and D-alanine:D-alanine ligase (DD-ligase) from *E. coli* (Fan *et al.*, 1994).

Among the cytoplasmic steps involved in the biosynthesis of peptidoglycan, four ADP-forming ligases catalyze the assembly of its peptide moiety by successive additions of L-alanine, D-glutamate, a diaminoacid (most frequently diaminopimelate or lysine) and D-alanyl-D-alanine to UDP-*N*-acetylmuramic acid (Rogers *et al.*, 1980; van Heijenoort, 1994). In *E. coli*, each of these steps is catalyzed by a unique ADP-forming ligase which are, respectively, the products of the *murC*, *murD*, *murE* and *murF* genes located in the *mra* region. Sequence comparisons among the four *E. coli* ADP-forming ligases show two homologous regions (Ikeda *et al.*, 1990b), suggesting that these enzymes may be evolutionarily related, and may use similar enzymatic mechanisms. The UDP-*N*-acetylmuramoyl-L-alanine: D-glutamate ligase, henceforth referred to as MurD, is of particular interest since the L-Ala-D-Glu linkage is present in the peptidoglycan of all eubacteria (Schleifer and Kandler, 1972; van Heijenoort, 1994). MurD catalyzes the addition of D-glutamate to the nucleotide precursor according to the following reaction:



The reaction has been proposed to proceed by phosphorylation of the C-terminal carboxylate of UDP-MurNAc-L-alanine by the γ -phosphate of ATP to form an acyl phosphate intermediate, followed by the nucleophilic attack by the amide group of the D-glutamate to produce UDP-MurNAc-L-Ala-D-Glu, ADP and inorganic phosphate (Vaganay *et al.*, 1996). This mechanism is supported further by the effectiveness of phosphinate transition-state analogs as inhibitors of MurD (Tanner *et al.*, 1996).

MurD from *E. coli* is a 47 kDa protein expressed in the cytoplasm as a single-chain monomer of 437 amino acids. The recombinant protein has been overproduced and purified to homogeneity (G. Auger, L. Martin, J. Bertrand, E. Fanchon, S. Vaganay, Y. Pétilot, J. van Heijenoort, D. Blanot and O. Dideberg, in preparation). The enzyme activity has been shown to be maximal in the presence of magnesium and phosphate ions. Nucleotide sequences of *murD* have been reported for *E. coli* (Mengin-Lecreulx *et al.*, 1989), *Bacillus subtilis* (Henriques *et al.*, 1992) and *Haemophilus influenzae* (Fleischmann *et al.*, 1995). Sequence identities with the enzyme from *E. coli* are 31% for *B. subtilis* and 62% for *H. influenzae*. This report describes the crystal structure of *E. coli* MurD in the presence of the substrate UDP-MurNAc-L-Ala (UMA). The structure reveals a three domain topology of the enzyme, allows the location of the active site and identifies the residues involved in UMA binding. It is the first structure reported for a member of the Mur ligase family,

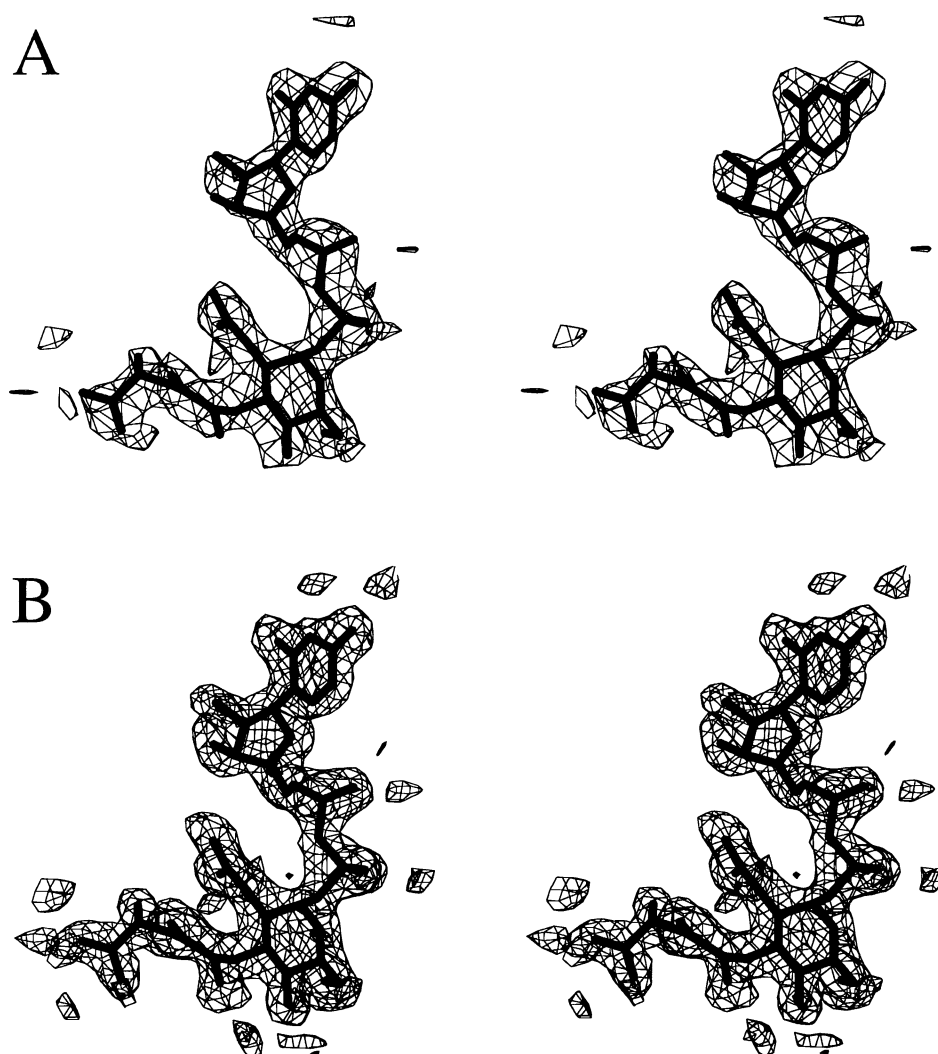


Fig. 1. Electron density around the substrate UDP-*N*-acetylmuramoyl-L-alanine (UMA) is superimposed on the final atomic model. (A) The original experimental map based on the MAD-MIR phases to 2.8 Å contoured at 1.7 σ . (B) The $(2F_o - F_c)$ map using phases from the final native MurD model to 1.9 Å contoured at 1 σ .

which includes the products of the *murC*, *murD*, *murE* and *murF* genes.

Results and discussion

Structure determination

The native and selenomethionyl MurD were expressed, purified and crystallized as reported elsewhere (G.Auger, L.Martin, J.Bertrand, E.Fanchon, S.Vaganay, Y.Pétillot, J.van Heijenoort, D.Blanot and O.Dideberg, in preparation). Mass spectroscopic analysis showed that all of the methionines were replaced by selenomethionines. In the crystals of selenomethionyl MurD, the 12 selenium atoms within the asymmetric unit provided a suitable means of obtaining experimental phasing information by taking advantage of the large anomalous features close to the selenium K-shell edge. Additional experimental phasing information was provided by co-crystals of selenomethionyl MurD with two different heavy atom derivatives, mercury acetate and 5-iodo-UMA. A combination of multiple anomalous dispersion (MAD) and multiple isomorphous replacement (MIR) phasing yielded a good

quality electron density map (Figure 1A), allowing the fitting of the polypeptide chain of MurD. The initial electron density can be compared with the corresponding $(2F_o - F_c)$ map (Figure 1B) after the final refinement. The selenomethionyl MurD model, refined to 2.8 Å resolution, was used subsequently to refine the structural parameters against 1.9 Å data collected from the native MurD.

The final model, which includes 430 residues, the substrate UMA, two sulfate molecules and 292 water molecules, has a crystallographic *R*-factor of 19.0% ($R_{\text{free}} = 23.5\%$; Brünger, 1992b) for all 34 834 reflections in the resolution range 8.0–1.95 Å (Table I). The root mean square (r.m.s.) deviations are 0.01 Å from ideal bond lengths and 1.3° from ideal bond angles. The Ramachandran plot (Ramachandran *et al.*, 1963) for the present model shows 92.2% of the residues in the most favored regions and none of the non-glycine residues in disallowed regions. The average temperature factor for the substrate UMA is 10.36 Å² and for the polypeptide chain backbone atoms is 11.95 Å². Two loops within the structure, residues 221–225 and 241–244, have no visible electron density and thus were not included in the model.

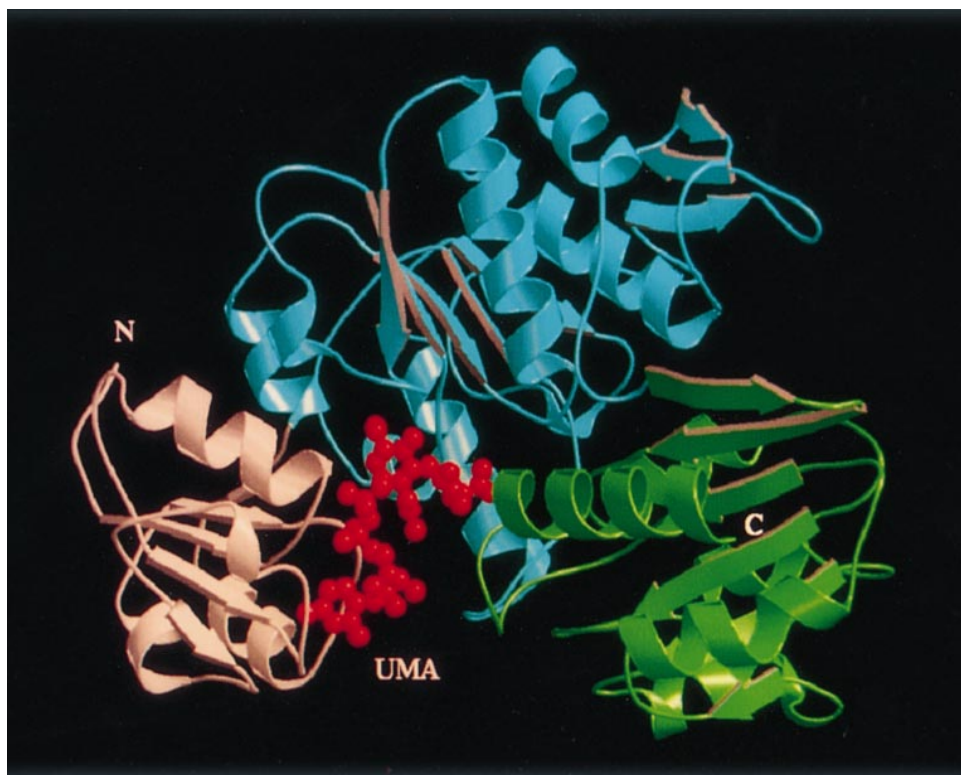


Fig. 2. Ribbon diagram of the binary complex of MurD and UMA produced with the program Molscript (Kraulis, 1991). Domain 1 is shown in pink, domain 2 in blue, domain 3 in green and UMA in red. For reasons of continuity, the two missing loops in the structure, residues 221–225 and 241–244, are shown interconnected in the figure.

Two cysteine residues, Cys208 and Cys227, were observed as partially oxidized. Two conformations of the cysteine side chains were built into the electron density and a partial occupancy was refined for the side chain atoms.

Overall protein structure

MurD consists of three globular domains formed from contiguous segments in the amino acid sequence (Figure 2). Domain 1 comprises residues 1–93 and consists of a five stranded parallel β -sheet surrounded by four helices. This domain accounts for the fixation of the UDP moiety of UMA. The topology of the domain (Figure 3A) is consistent with the classic ‘dinucleotide-binding fold’ of dehydrogenases, also called the Rossmann fold (Rossmann *et al.*, 1975; Schulz, 1992), except that MurD lacks the fifth helix, and the sixth and final β -strand. The short loop (P-loop) between β 1 and α 1 is responsible for the binding of the phosphates of UMA. Comparison of the domain 1 structure with the known database of protein structures carried out with the program SARF (Alexandrov and Go, 1994) reveals, as expected, many Rossmann folds. The structure with highest similarity is glycinamide ribonucleotide transformylase (Klein *et al.*, 1995) with an r.m.s. deviation of 2.71 Å for the 83 structurally equivalent C α atoms.

Domain 2 (Figure 3B) comprises residues 94–298 and consists of a central six stranded parallel β -sheet surrounded by seven α -helices with a small flanking three stranded antiparallel β -sheet. The fold of the central β -sheet is similar to the classic ‘mononucleotide-binding fold’ as found in many ATP- and GTP-binding proteins.

Table I. Quality of the final model

Crystallographic <i>R</i> -value (%)	19.0
No. of reflections	34 834
Resolution range (Å)	8–1.95
R.m.s. deviations from standard geometry	
Bond length (Å)	0.01
Bond angles (°)	1.3
Dihedral angles (°)	25.5
Improper angles (°)	2.27
No. of non-hydrogen atoms	
Protein	3222
UMA	49
Water	294
Sulfate	90
Average <i>B</i> -value (Å ²)	
All atoms	13.97
Protein atoms	13.23
UMA	10.36
Water molecules	22.21
Sulfate molecules	27.64
Backbone atoms	11.81

This domain 2 will therefore be referred to as the GTPase domain. A significant number of protein structures of the so-called GTPase family have now been reported, including adenylate kinase (ADK; Diederichs and Schulz, 1990), ras P21 (Pai *et al.*, 1989), elongation factors Tu (EF-Tu; Berchtold *et al.*, 1993), transducin G_{t α} (Noel *et al.*, 1993), adenylosuccinate synthetase (Poland and Honzatko, 1993) and dethiobiotin synthetase (Alexeev *et al.*, 1994; Huang *et al.*, 1994). The loop between β 6 and α 6 of the GTPase domain is believed to be involved

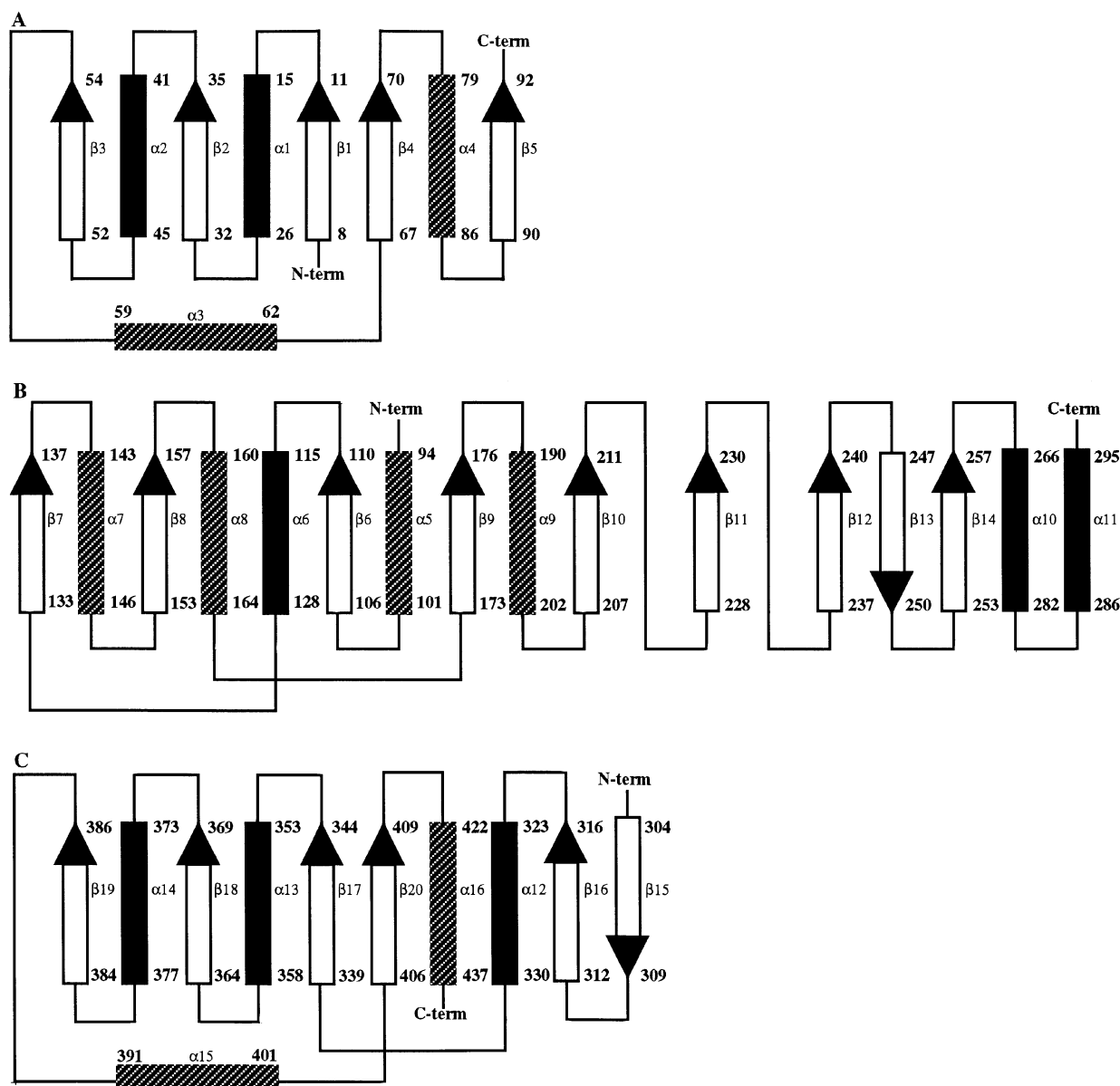


Fig. 3. Schematic diagram of the polypeptide topology of the three domains of MurD. The β -strands are depicted as arrows, with the arrowheads indicating the direction of the chain. α -Helices below and above the β -sheet are represented by shaded and black rectangles, respectively.

in the ATP fixation. This domain is also responsible for the remainder of the UMA interactions, accounting for the fixation of the muramic acid and L-alanine moieties of UMA.

Domain 3 (299–437) contains a six stranded β -sheet with parallel strands (β 16, β 17, β 18, β 19 and β 20) and an antiparallel strand (β 15), and five surrounding α -helices (Figure 3C). Domain 3 is larger than domain 1 but, surprisingly, also contains a Rossmann fold. As shown in Figure 3, β 1, α 1, β 2, α 2, β 3, α 3, β 4 and α 4 of domain 1 correspond to β 17, α 13, β 18, α 14, β 19, α 15, β 20 and α 16 of domain 3. Moreover, a superposition based on the four principal β -strands gives an r.m.s. deviation of 2.20 Å for the 96 structurally equivalent main chain atoms. Strands β 15 and β 16 and the helix α 12 have no structural equivalents in domain 1. Although the interconnectivity is different, strand β 16 of domain 3 occupies a position consistent with that of β 5 in domain 1.

Comparison with other ligases

For the peptide bond synthesis, both in ribosomes and in non-ribosomal multienzyme complexes, the enzymatic mechanism involves an aminoacyl-AMP intermediate. In contrast, a few peptide ligases use another mechanism in which ATP hydrolysis yields two products (ADP and P_i). For these enzymes, the carboxylate of the peptide is activated by the transfer of the phosphoryl group. The best characterized ligases or synthetases include glutamine synthetase (EC 6.3.1.2), γ -Glu-Cys synthetase (EC 6.3.2.2), glutathione synthetase (GSHase; EC 6.3.2.3), DD-ligase (EC 6.3.2.4), phosphoribosylaminoimidazole-succinocarboxamide synthetase (EC 6.3.2.6), the four Mur ligases (EC 6.3.2.8; 9; 13; and 15) and folsylpolyglutamate synthetase (EC 6.3.2.17). Among these synthetases, the X-ray structures have been determined for glutamine synthetase (Yamashita *et al.*, 1989), GSHase (Yamaguchi *et al.*, 1993) and DD-ligase (Fan *et al.*, 1994), all from

Table II. Hydrogen bonds involved in UMA binding

UMA residue	Atom	MurD residue	Atom	Distance (Å)
Ala	OA	His183	Nε2	2.7
		Wat600	O	2.8
		Wat712	O	2.6
Ala	OB	Asn138	Nδ2	3.0
Ala	N	Asn138	Oδ1	3.1
Amu	O18	Wat795	O	2.9
Amu	O4''	Asn138	O	2.7
		Wat594	O	2.8
Amu	N2''	Wat529	O	2.9
Amu	O7''	Wat565	O	2.6
Amu	O6''	Wat501	O	2.9
		Wat502	O	2.9
Udp	O2β	Thr16	Oγ1	2.6
		Thr16	N	2.8
Udp	O1β	Leu15	N	3.0
		Wat682	O	3.0
		Wat684	O	3.1
		Gly73	N	2.8
Udp	O2α	Arg37	NH2	3.1
		Wat554	O	2.9
Udp	O2'	Gly73	O	3.0
		Wat566	O	3.2
Udp	O4'	Arg37	NH1	2.9
Udp	N3	Thr36	Oγ1	2.8
Udp	O4	Thr36	N	3.0

E.coli. Although there is very little sequence homology between these proteins, the comparison of their three-dimensional structures reveals a similarity in the spatial arrangement of the secondary structure elements (Fan *et al.*, 1995) between the DD-ligase and the GSHase. Moreover, a set of 13 spatially equivalent residues, mainly forming the ATP-binding site, strongly supports a family relationship between these two enzymes. Recently, another unsuspected evolutionary relationship was observed between DD-ligase, GSHase and biotin carboxylase (Artymiuk *et al.*, 1996). As observed for the previous enzymes, MurD also has a three domain organization, but none of the domains has a tertiary structure similar to that of the other known ligase structures. As a result, MurD is believed to be the first example of a new family of ADP-forming ligases.

UMA binding

The substrate UMA binds to MurD in the cleft formed between domain 1 and the GTPase domain. After density modification using DM (CCP4, 1994), the MAD-MIR electron density clearly showed the entire UMA molecule (Figure 1A). As listed in Table II, the bound UMA forms many polar interactions with the protein. Domain 1 residues implicated in the UMA fixation are located in the loop connecting β1 with α1 and the two loops at the end of the adjacent strands β2 and β4. As can be seen from the electron density (Figure 1B), the geometry of the uridine-ribose moiety of UMA is *C₂'-endo* for the ribose ring pucker and *anti* orientation about the glycosyl bond. The uracyl ring of UMA forms two hydrogen bonds with Thr36: O4 with the main chain nitrogen and N3 with Oγ. In addition, the uracyl ring participates in interplane stacking with a salt bridge formed between Asp35 and Arg37. A weak hydrogen bond is also formed between NH1 of Arg37 and O4' of the ribose. The hydroxyl group

in the O2' position of the ribose forms hydrogen bonds with the carbonyl oxygen of Gly73 and a water molecule.

The pyrophosphate of UMA is located in the loop connecting β1 with α1 (residues 12–17). The sequence of this 'P-loop', Gly-Leu-Gly-Leu-Thr-Gly, is consistent with the characteristic dinucleotide-binding fingerprint sequence. The protein-phosphate interactions are mainly through hydrogen bonds with main chain nitrogens; the α-phosphate oxygens make hydrogen bonds with Gly73 and the β-phosphate oxygens with Leu15 and Thr16 of the P-loop. One of the β-phosphate oxygens hydrogen bonds with the side chain oxygen of Thr16 and the other hydrogen bonds with two water molecules. Furthermore, one of the α-phosphate oxygens also forms hydrogen bonds with NH2 of Arg37, and with Wat554. As mentioned above, Arg37 also forms a salt bridge with Asp35, presumably balancing the two charged groups. As a result, no charged side chains are available to balance the negative charge of the phosphates, which is presumably accommodated by the helix dipole of α1 (Wierenga *et al.*, 1985).

The *N*-acetylmuramic acid ring bridges the gap between domain 1 and the GTPase domain, forming hydrogen bonds with the carbonyl oxygen of Asn138 and several water molecules. Side chain atoms of Asn138 also participate in hydrogen bonds with the L-alanine of UMA; Oδ1 hydrogen bonds with the backbone nitrogen of L-alanine and Nδ2 hydrogen bonds with OB of the L-alanine carboxylate. The other UMA carboxylate atom, OA, forms hydrogen bonds with Nε2 of His183 and two water molecules (Wat600 and Wat712).

ATP-binding site

In nucleotide-binding proteins with the classical mononucleotide fold, there is a characteristic fingerprint, Gly-X-X-Gly-X-Gly-Lys-Thr/Ser (Walker *et al.*, 1982; Saraste *et al.*, 1990), located in a loop between a central β-strand and an α-helix. A large anion hole is formed by the loop which accommodates the phosphates of the mononucleotide (Dreusicke and Schulz, 1986). In the MurD structure, this loop comprises residues 108–116 with the sequence Ala-Ile-Thr-Gly-Ser-Asn-Gly-Lys-Ser. It contains an additional residue inserted between the second and third glycine residues of the motif and is located between β6 and α6 of the GTPase domain. By analogy with other ATP-binding proteins, the sulfate molecule sitting at the N-terminal end of α6 is believed to be consistent with the position of the α-phosphate of ATP. Residues coordinating and stabilizing the sulfate molecule include Arg302, Lys319, Thr117, Gly114 and Asn113. A bridging water molecule is located between one of the sulfate oxygens and the terminal nitrogen of Lys115. In order to locate the ATP-binding cleft in MurD, the P-loops of ras p21 complexed with a GTP analog (Pai *et al.*, 1990) and that of dethiobiotin synthetase complexed with the substrate 7,8-diaminononanoic acid, an ATP analog and Mn²⁺ ion (Huang *et al.*, 1995) were superimposed on the P-loop of MurD (Figure 4). Functionally equivalent molecules or ions, when present, are observed in similar positions: UMA and 7,8-diaminononanoic acid (MurD and dethiobiotin synthetase); Mg²⁺ and Mn²⁺ ions (ras p21 and dethiobiotin synthetase); GTP and ATP analogs (ras p21 and dethiobiotin synthetase); SO₄²⁻ ion and α-phosphate of the GTP/

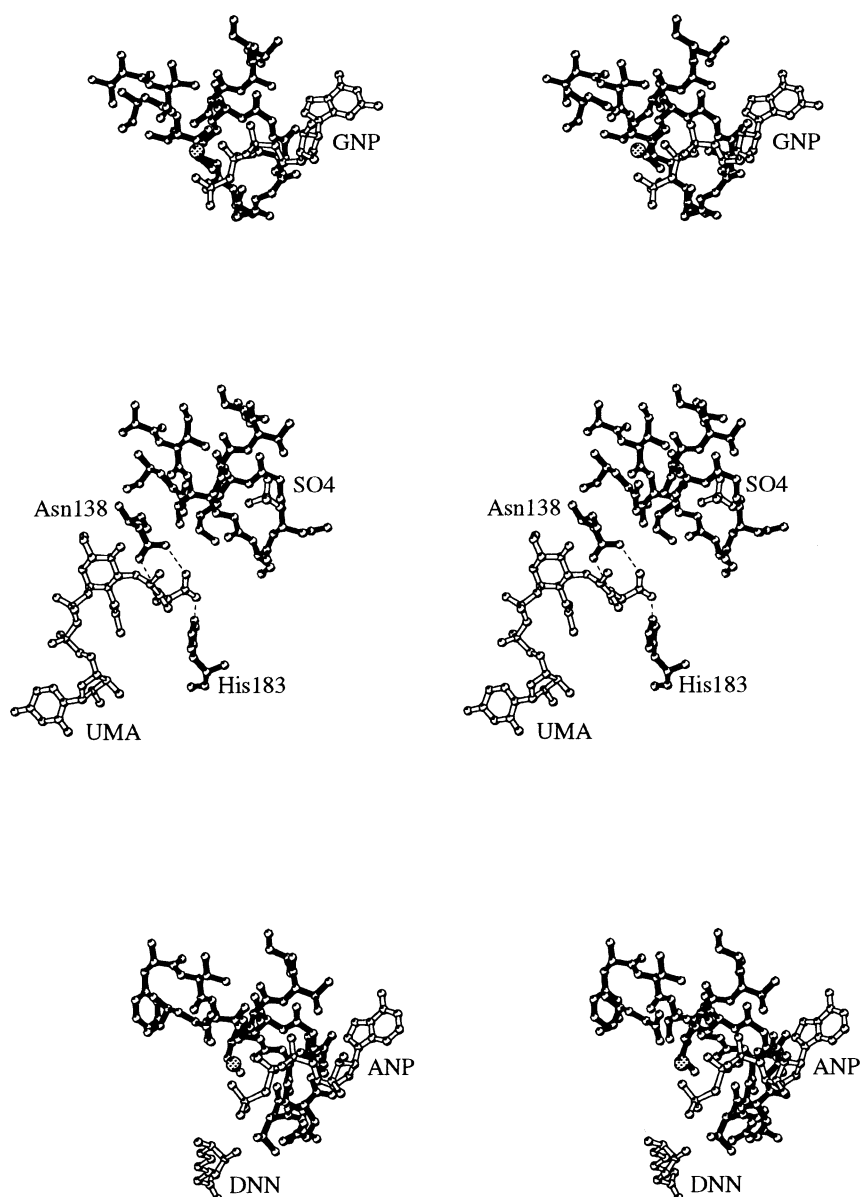


Fig. 4. Stereo views of the P-loops of the Ha-ras oncogene product p21 (Pai *et al.*, 1990; PDB entry 5P21), *E.coli* dethiobiotin synthetase (Huang *et al.*, 1995; PDB entry 1DAH) and MurD determined by optimal C α superposition. (A) The Ha-ras p21 structure includes p21 residues 7–19, 57, the GTP analog guanosine 5'-(β,γ -imido) triphosphate (GNP) and the Mg²⁺ ion. (B) The MurD structure includes residues 108–118, 138, 157, 183, the substrate UDP-MurNAc- L-Ala (UMA) and the sulfate ion. (C) The dethiobiotin synthetase structure includes residues 5–18, 115, the substrate 7,8-diaminononanoic acid (DNN), the ATP analog adenylyl (β,γ -methylene) diphosphonate (ANP) and the Mn²⁺ ion.

ATP analog (MurD and ras p21/dethiobiotin synthetase). While detailed statements concerning ATP fixation must await a structure of the complex with the nucleotide, certain residues which may be involved can be identified from the superpositions. In the current MurD structure, the residues involved in the fixation of SO₄²⁻ are believed to play a role in fixation of the ATP phosphates, the salt bridge formed between Arg302 and Asp317 is most likely displaced by the ATP ribose moiety, and the side chain positions of Asn268 and Asn271 make them likely participants in the fixation of the adenine moiety.

Many of the enzymes containing the P-loop contain a divalent cation pocket, with one ligand supplied by the conserved hydroxyl residue at the last position of the P-loop (Ser116 in MurD) and another supplied by an acidic residue at the C-terminal end of the adjacent β -strand.

Enzymatic assays have shown that the cation is required for full activity of MurD (Pratviel-Sosa *et al.*, 1991). A search of the MurD structure in the vicinity of Lys115, the conserved P-loop residue implicated in the fixation of the β - and γ -phosphates, shows the side chain of Glu157 directed towards the ATP-binding site. It is presumed that, in the presence of ATP, this acidic residue plays a role in Mg²⁺ fixation.

Homology with other *E.coli* ligases

Sequence homology has been reported previously for the four ligases of *E.coli*: MurC, MurD, MurE and MurF (Ikeda *et al.*, 1990b). Using the structural information obtained for MurD, the alignment of the four enzymes was repeated moving potential insertions into loop regions whenever possible. For regions where the sequence

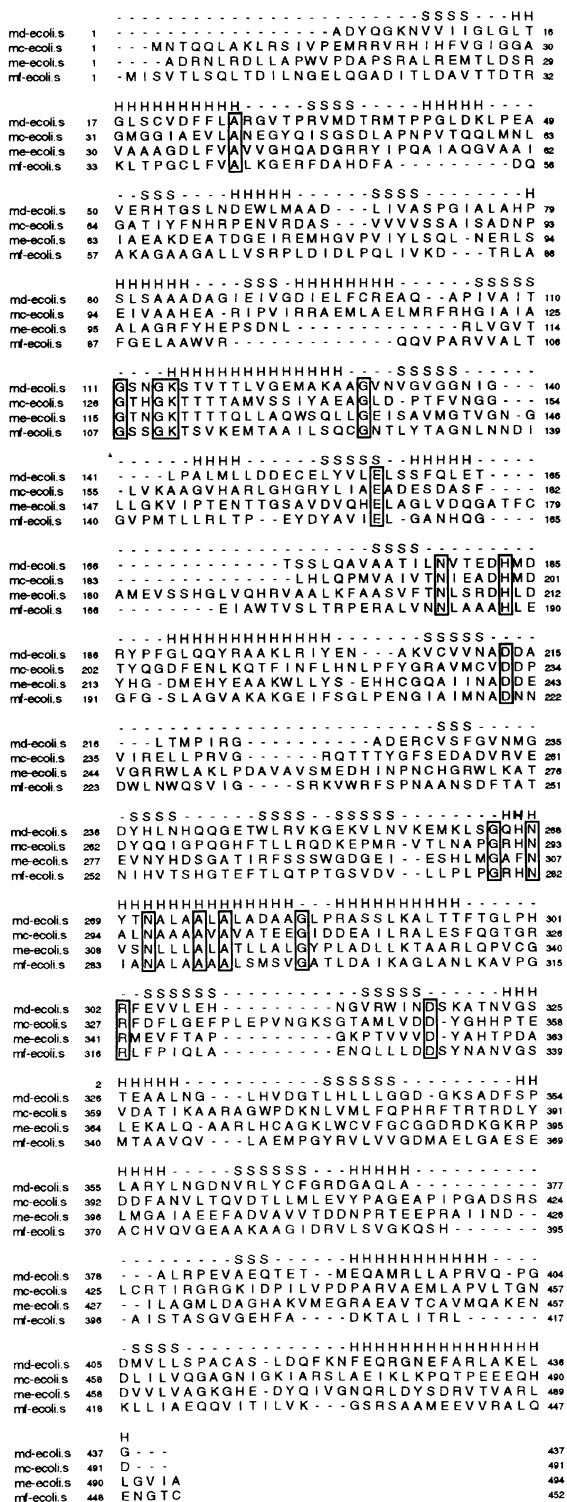


Fig. 5. Amino acid sequence alignment of members of the Mur ligase family from *E. coli*. The figure was produced with the program SeqVu. The first line shown secondary structure elements observed in the 3D structure. Residues are marked with an H or an S, depending on whether they belong to an α -helix or a β -sheet, respectively. Sequences used for the alignment are: md-ecoli.s (Mengin-Lecreulx and van Heijenoort, 1990), mc-ecoli.s (Ikeda *et al.*, 1990a), me-ecoli.s (Michaud *et al.*, 1990) and mf-ecoli.s (Parquet *et al.*, 1989). Conserved residues in the four sequences are boxed.

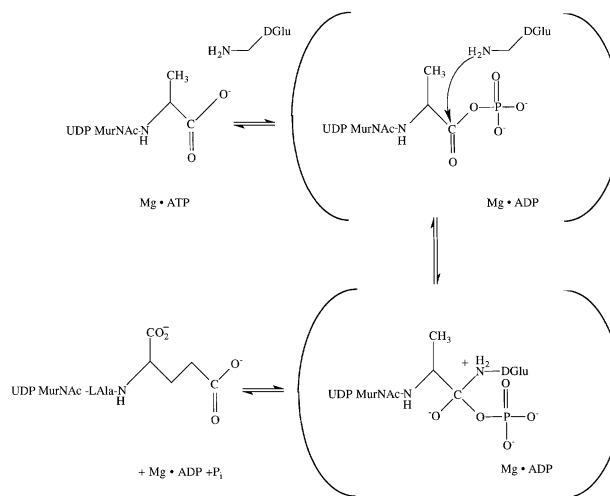


Fig. 6. Proposed catalytic mechanism for the formation of UDP-*N*-acetylmuramoyl-L-alanine-D-glutamate by MurD.

similarity is very weak, mainly in domains 1 and 3, the alignment was made using the hydrophobic cluster analysis program (HCA; Gaboriaud *et al.*, 1987). The results are shown in Figure 5. A striking feature of the alignment is the conservation, in all four ligases, of residues which are in interaction with the substrates and are presumably important for activity: Gly114, Lys115, Ser or Thr116, Glu157, His183, Asn268, Asn271, Arg302 and Asp317.

Structural implications for catalysis

In general, ATP-dependent amide-forming enzymes are believed to share a common mechanism by catalyzing an initial phosphorylation of the acid carboxylate. Subsequently, the resulting acyl phosphate is attacked by the amine, producing a tetrahedral intermediate which ultimately collapses to the final product and inorganic phosphate (Figure 6). In order for the ligation to occur between UMA and D-Glu, the enzyme MurD must (i) bring together the UMA and ATP, (ii) properly orient UMA and ATP for the formation of an acyl-phosphate intermediate, (iii) orient D-Glu for the nucleophilic attack, and (iv) stabilize the tetrahedral intermediate, thereby lowering the activation barrier and accelerating catalysis. The structure determination of MurD has revealed the location of the active site and identified the protein residues involved in the fixation of the substrate UMA. In addition, the approximate location of the ATP-binding site has been determined by structural homology with other NTP-binding proteins and by the location of a sulfate molecule in the P-loop. The active site of MurD is located in the cleft between the GTPase domain and domain 3; the reactive part of UMA enters the cleft from the side closest to domain 1 and the ATP molecule from the opposite side. Residues involved in the fixation of UMA include Leu15, Thr16, Thr36, Arg37, Gly73, Asn138 and His183. GTPase domain residues Asn138 and His183 are within hydrogen bonding distance of the carboxylate oxygens OB and OA, respectively. Orientation and nearest-neighbor considerations suggest that the acyl phosphate is formed with UMA carboxylate oxygen OB, implicating Asn138 as a likely participant in the formation of the acyl phosphate. His183 would serve a role in orienting the carboxylate group prior to phosphorylation.

Table III. MurD data collection and phasing statistics

Crystal form	Seleno-MurD remote λ_1	Seleno-MurD inflection λ_2	Seleno-MurD peak λ_3	Seleno-MurD remote λ_4	Seleno-MurD HgAc MAR ^e	Seleno-MurD Iodo-UMA MAR	Native
X-ray source	ESRF	ESRF	ESRF	ESRF	MAR ^e	MAR	ESRF
Cell constants							
$a = b$ (Å)	65.5	65.5	65.5	65.5	65.6	65.7	65.4
c (Å)	134.6	134.6	134.6	134.6	134.7	134.7	134.4
Data collection							
Wavelength (Å)	0.9827	0.9797	0.9794	0.9762	1.5418	1.5418	1.0723
d_{\min} (Å)	2.7	2.7	2.7	2.7	2.9	2.0	1.9
No. of unique	14 298	14 345	14 354	14 343	12 699	36 626	38 921
Multiplicity	4.3	4.3	4.3	4.4	5.8	3.6	3.5
Completeness (%)	99.0 (97.6)	99.4 (98.8)	99.4 (98.7)	99.3 (98.4)	96.2 (85.3)	95.1 (87.9)	94.7 (79.7)
R_{sym} (%) ^a	3.7 (10.0)	4.4 (14.8)	4.4 (14.8)	4.5 (11.8)	9.6 (14.7)	11.7 (22.3)	6.5 (25.9)
Phasing							
No. of sites	12	12	12	12	13	13	
R_{cullis} acentric (%) ^b	60		64	64	71	93	
Phasing power acentric ^c	1.89		1.68	1.62	1.52	0.64	
R_{cullis} anomalous (%) ^d	93	64	56	65			

Numbers in parentheses correspond to the shell of data at highest resolution.

^a $R_{\text{sym}} = \sum_{\text{hi}} |I(h) - I(h)_i| / \sum_{\text{hi}} I(h)_i$ where $I(h)$ is the mean intensity after rejections.

^b R_{cullis} acentric = r.m.s. lack of closure/r.m.s. isomorphous difference.

^cPhasing power = $\langle |F_H| \rangle / \text{r.m.s. lack of closure for acentric reflections}$.

^d R_{cullis} anomalous = r.m.s. lack of closure/r.m.s. anomalous difference.

^eMAR, in house X-ray generator (RIGAKU RU200).

Materials and methods

Preparation of 5-iodoUDP-MurNAc-L-Ala

5-Iodo-UMA was synthesized from UMA by mercuration of the uracil moiety followed by iodination, according to Dale *et al.* (1973, 1975).

UMA (5 μmol) was dissolved in 0.1 M sodium acetate buffer, pH 6.0 (0.25 ml). Mercuric acetate (25 μmol), dissolved in the same buffer (0.25 ml), was added, and the mixture was heated at 50°C for 5 h. High performance TLC (HPTLC) on silica gel 60F₂₅₄ (Merck) in ethanol: 1 M ammonium acetate 7:3 (v/v) showed the complete transformation of the starting material ($R_f = 0.62$) into a new compound ($R_f = 0.49$). Gel filtration on Sephadex G-25 in water afforded 5-mercuri-UMA, which displayed a single spot in HPTLC. Its yield (3.5 μmol , 70%) was estimated by using an ϵ_M value of 10 100M⁻¹ cm⁻¹ at 267 nm (Dale *et al.*, 1973).

The synthesis of another mercurated derivative was attempted by reaction of this compound with ethanethiol; however, the product formed ($R_f = 0.73$, presumably 5-ethylthiomercuri-UMA) decomposed back to 5-mercuri-UMA and UMA upon storage.

To 5-mercuri-UMA (1.75 μmol) dissolved in water (0.14 ml), potassium iodide (0.23 ml of a 50 mM aqueous solution) and iodine (6.5 μl of a 788 mM ethanolic solution) were added. The mixture was allowed to stand for 3 h at room temperature. HPTLC in the above conditions showed the appearance of a new compound ($R_f = 0.93$), with traces of the starting material remaining. Reverse-phase HPLC on Vydac 218TP in 50 mM ammonium formate, pH 3.9, afforded 5-iodo-UMA which displayed a single spot in HPTLC. Its yield (1.2 μmol , 69%) was estimated by using an ϵ_M value of 8000 M⁻¹ cm⁻¹ at 289 nm (Michelson *et al.*, 1962). Plasma-desorption mass spectrometry in the negative mode showed the molecular ion (m/z 875) together with fragments corresponding to the loss of iodine (m/z 749), of MurNAc-L-Ala (m/z 529), and of iodine plus MurNAc-L-Ala (m/z 403).

The ability of the synthesized compounds to behave as substrates for MurD was tested under the previously published conditions (Vaganay *et al.*, 1996). 5-Iodo-UMA was a good substrate, with a K_M value of $2.7 \pm 0.8 \mu\text{M}$ (K_M for UMA in the same conditions: $3.2 \pm 0.7 \mu\text{M}$). 5-Mercuri-UMA was not a substrate but, after pre-incubation (5 min) in the absence of reducing agent, it strongly inhibited the enzyme ($\text{IC}_{50} = 0.29 \mu\text{M}$).

Data collection and processing

A detailed description of the MurD expression, purification and crystallization will be reported elsewhere (G.Auger, L.Martin, J.Bertrand, E.Fanchon, S.Vaganay, Y.Pétilot, J.van Heijenoort, D.Blanof and O.Dideberg, in preparation). The binary enzymatic complex was formed by mixing MurD with a 5-fold excess of UMA. Tetragonal crystals

(space group P4₁ or P4₃) of native and selenomethionyl MurD in the presence of UMA were grown at pH 7.2. The crystals have unit cell dimensions $a = b = 65.50$ and $c = 134.59$ Å, diffract to Bragg spacing of 1.95 Å and have one molecule per asymmetric unit. All data were collected at 100 K from crystals with typical dimensions of 0.5×0.2×0.2 mm (Table III). Native data to 1.95 Å and selenomethionine MAD data to 2.77 Å were collected on the D2AM beamline, at the European Synchrotron Radiation Facility (ESRF, Grenoble, France), using a detection system based on a CCD camera coupled to an image intensifier (Moy, 1994). Integration of the D2AM data was done with a version of the program XDS (Kabsch, 1988) which has been adapted by the author to the CCD detector. Whenever not specified otherwise, the data were scaled and merged using the CCP4 programs ROTAVATA and AGROVATA (CCP4, 1994).

MAD data, at four wavelengths, were measured from a single frozen selenomethionyl MurD crystal. The wavelengths, near the K-shell edge of selenium, were chosen from an X-ray fluorescence spectrum from the frozen MurD crystal. Next, the crystal was oriented so that Bijvoet mates were measured simultaneously. To ensure the best consistency of the data for the phase determination, X-ray data were collected at all four wavelengths in 10° sectors (exposure time = 10 s, image width = 0.5°). A total of 110° were collected with the crystal 'oriented' followed by 30° with the crystal 'offset'. Derivative data were collected on a MarResearch imaging plate system using X-rays provided by a Rigaku RU-200 and integrated with MAR_XDS (Kabsch, 1988). The 5-iodo-UMA derivative and mercury derivative were both prepared by co-crystallization of selenomethionyl MurD with the corresponding reagent: 1 mM 5-iodo-UMA in place of UMA or the addition of 1 mM mercuric acetate.

Phase determination

The algebraic method as implemented by Hendrickson (Hendrickson *et al.*, 1988) was applied to locate the selenium atoms (programs cited below without reference are part of Hendrickson's MADSYS package). The steps involved in deriving phases are: local scaling (between Bijvoet mates at one wavelength, ANOSCL, and between different wavelengths, WVLSCL), resolution of the phasing equations (MADLSQ), merging of equivalent observations (MERGIT), location of the anomalous scatterers, refinement of anomalous scattering parameters and calculation of phase probabilities.

Using the MADLSQ procedure, it is possible to derive the moduli of structure factors for normal scattering from the entire structure, $|F_T|$, those from the anomalous scatterers (here the selenium atoms), $|F_A|$, and the phase differences $\Delta\phi = \phi_T - \phi_A$. Initial values for f' and f'' , at the four chosen wavelengths, were derived from the fluorescence scan (XASFIT, KRAMIG). Several rounds of MADLSQ/MERGIT were

performed with different values of wavelength scales and anomalous scattering factors f' and f'' . Trial values for f' and f'' were taken from the fluorescence scan assuming that a slight shift in wavelength had taken place. The combination giving the best indicators after merging (average redundancy = 4.3) was kept: $R_{\text{sym}}(|F_{\text{T}}|) = 4.7\%$, $R_{\text{sym}}(|F_{\text{A}}|) = 31.6\%$, and $\langle \Delta(\Delta\phi) \rangle = 27.9^\circ$. The total number of observed phasing sets was 33 667, of which 3% were left unphased by MADLSQ, yielding 13 725 unique reflections after merging. Direct methods (Sheldrick, 1990) were then used on the averaged F_{A} moduli to locate the selenium sites. A well contrasted list of 12 peaks was obtained after rejection of outliers from the F_{A} set. These sites were refined against the F_{A} moduli with ASLSQ. The last step, refinement of the 'heavy-atom' parameters with calculation of the phase probabilities, was performed with MLPHARE (CCP4, 1994), treating the 0.9797 Å data set as the 'native' data (Ramakrishnan *et al.*, 1993).

The iodine and mercury positions were located in difference Fourier maps made using MAD-derived phases. Combined MIR- and MAD-derived phases were calculated using reflections from 30.0 to 2.77 Å resolution in both space group enantiomorphs P4₁ and P4₃. A clear solvent boundary was observed in the electron density map in space group P4₁. Density modification was applied to improve the initial phases using DM (CCP4, 1994).

Model building and refinement

The polypeptide chain of MurD was traced using an Evans and Sutherland workstation running the program O (Jones *et al.*, 1991). The selenium sites provided markers for the methionine side chains and facilitated the assignment of the amino acid sequence in the electron density map. For refinement purposes, the small Bijvoet differences at the first wavelength of the MAD data, 0.9827 Å, were ignored and the data was reprocessed as if there was no anomalous scattering contribution. Least squares and simulated annealing refinement of the selenomethionyl MurD were carried out using X-PLOR (Brünger, 1992b), resulting in an R -factor of 24.1% ($R_{\text{free}} = 33.2\%$; Brünger, 1992a) for data between 8.0 and 2.8 Å. Subsequent refinement used the resulting model to refine against data collected from native MurD at 1.95 Å resolution. Several cycles of refinement and manual rebuilding provided a model containing 3598 non-hydrogen atoms including the substrate UMA, two SO_4^{2-} ions and 292 water molecules. This model has a crystallographic R -factor of 19.0% for all 34 834 reflections in the resolution range of 8.0–1.95 Å. An R_{free} of 23.5% was obtained from a 5% subset of the data which was excluded from the refinement. The final coordinates of the MurD structure have been deposited with the Brookhaven Protein Data Bank (accession code 1UAG) and will be released 1 year after publication.

In order to judge objectively the quality of the electron density maps calculated with the MIR- and MAD-derived phases, we calculated the correlation between the various maps and a map calculated with the final selenomethionyl MurD model using the program OVERLAPMAP (CCP4, 1994). The MAD data at 0.9827 Å were used for the correlation, giving values of 0.66 before and 0.84 after density modification.

Acknowledgements

We wish to thank M.Roth (IBS, LCCP) for assistance in data collection, R.Kahn for assistance in data treatment and E.Duée for preliminary tests on the SHELXS-90 program. This work was supported by grants from the Centre National de la Recherche Scientifique (URA 1131) and the Action Concertée Coordonnée Sciences du Vivant (No. V). This is publication No. 438 of the Institut de Biologie Structurale Jean-Pierre Ebel (CEA-CNRS).

References

Alexandrov,N.N. and Go,N. (1994) Biological meaning, statistical significance, and classification of local spatial similarities in nonhomologous proteins. *Protein Sci.*, **3**, 866–875.
 Alexeev,D., Baxter,R.L. and Sawyer,L. (1994) Mechanistic implications and family relationships from the structure of dethiobiotin synthetase. *Structure*, **2**, 1061–1072.
 Artymiuk,P.J., Poirrette,A.R., Rice,D.W. and Willett,P. (1996) Biotin carboxylase comes into the fold. *Nature Struct. Biol.*, **3**, 128–132.
 Benson,T.E., Filman,D.J., Walsh,C.T. and Hogle,J.M. (1995) An enzyme–substrate complex involved in bacterial cell wall biosynthesis. *Nature Struct. Biol.*, **2**, 644–653.

Berchtold,H., Reshetnikova,L., Reiser,C.O.A., Schirmer,N.K., Sprinzl,M. and Hilgenfeld,R. (1993) Crystal structure of active elongation factor Tu reveals major domain rearrangements. *Nature*, **365**, 126–132.
 Brünger,A.T. (1992a) *X-PLOR Version 3.1: A System for X-ray Crystallography and NMR*. Yale University Press, New Haven, CT.
 Brünger,A.T. (1992b) Free R value: a novel statistical quantity for assessing the accuracy of crystal structures. *Nature*, **355**, 472–475.
 CCP4 (1994) The CCP4 suite: programs for protein crystallography. *Acta Crystallogr.*, **D50**, 760–763.
 Dale,R.M.K., Livingston,D.C. and Ward,D.C. (1973) The synthesis and enzymatic polymerization of nucleotide containing mercury: potential tools for nucleic acid sequencing and structural analysis. *Proc. Natl Acad. Sci. USA*, **70**, 2238–2242.
 Dale,R.M.K., Martin,E., Livingston,D.C. and Ward,D.C. (1975) Direct covalent mercuration of nucleotides and polynucleotides. *Biochemistry*, **14**, 2447–2457.
 Diederichs,K. and Schulz,G.E. (1990) Three-dimensional structure of the complex between the mitochondrial matrix adenylate kinase and its substrate AMP. *Biochemistry*, **29**, 8138–8144.
 Dreusicke,D. and Schulz,G.E. (1986) The glycine-rich loop of adenylate kinase forms a giant anion hole. *FEBS Lett.*, **208**, 301–304.
 Fan,C., Moews,P.C., Walsh,C.T. and Knox,J.R. (1994) Vancomycin resistance: structure of D-alanine: D-alanine ligase at 2.3 Å resolution. *Science*, **266**, 439–443.
 Fan,C., Moews,P.C., Shi,Y., Walsh,C.T. and Knox,J.R. (1995) A common fold for peptide synthetases cleaving ATP to ADP: glutathione synthetase and D-alanine: D-alanine ligase of *Escherichia coli*. *Proc. Natl Acad. Sci. USA*, **92**, 1172–1176.
 Fleischmann,R.D. *et al.* (1995) Whole-genome random sequencing and assembly of *Haemophilus influenzae* Rd. *Science*, **269**, 496–512.
 Gaboriaud,C., Bissery,V., Bencherit,T. and Mornon,J.P. (1987) Hydrophobic cluster analysis: an efficient new way to compare and analyse amino acid sequences. *FEBS Lett.*, **224**, 149–155.
 Hendrickson,W.A., Smith,J.L., Phizackerley,R.P. and Merritt,E.A. (1988) Crystallographic structure analysis of lamprey hemoglobin from anomalous dispersion of synchrotron radiation. *Proteins: Struct. Funct. Genet.*, **4**, 77–88.
 Henriques,A.O., de Lencastre,H. and Piggot,P.J. (1992) A *Bacillus subtilis* morphogene cluster that includes *spoVE* is homologous to the *mra* region of *Escherichia coli*. *Biochimie*, **74**, 735–748.
 Huang,W., Lindqvist,Y., Schneider,G., Gibson,K.J., Flint,D. and Lorimer,G. (1994) Crystal structure of an ATP-dependent carboxylase, dethiobiotin synthetase, at 1.65 Å resolution. *Structure*, **2**, 407–414.
 Huang,W., Jia,J., Gibson,K.J., Taylor,W.S., Rendina,A.R., Schneider,G. and Lindqvist,Y. (1995) Mechanism of an ATP-dependent carboxylase, dethiobiotin synthetase, based on crystallographic studies of complexes with substrates and a reaction intermediate. *Biochemistry*, **34**, 10985–10995.
 Ikeda,M., Wachi,M., Ishino,F. and Matsuhashi,M. (1990a) Nucleotide sequence involving *murD* and an open reading frame ORF-Y spacing *murF* and *ftsW* in *Escherichia coli*. *Nucleic Acids Res.*, **18**, 1058.
 Ikeda,M., Wachi,M., Jung,H.K., Ishino,F. and Matsuhashi,M. (1990b) Homology among MurC, MurD, MurE and MurF proteins in *Escherichia coli* and that between *E.coli* MurG and a possible MurG protein in *Bacillus subtilis*. *J. Gen. Appl. Microbiol.*, **36**, 179–187.
 Jones,T.A., Zou,J.-Y., Cowan,S.W. and Kjeldgaard,M. (1991) Improved methods for building protein models in electron density maps and the location of errors in these models. *Acta Crystallogr.*, **D47**, 110–119.
 Kabsch,W. (1988) Evaluation of single crystal X-ray diffraction data from a position sensitive detector. *J. Appl. Crystallogr.*, **21**, 916–924.
 Klein,C., Chen,P., Arevalo,J.H., Stura,E.A., Marolewski,A., Warren,M.S., Benkovic,S.J. and Wilson,I.A. (1995) Towards structure-based drug design: crystal structure of a multisubstrate adduct complex of glycinamide ribonucleotide transformylase at 1.96 Å resolution. *J. Mol. Biol.*, **249**, 153–175.
 Kraulis,P.J. (1991) MOLSCRIPT: a program to produce both detailed and schematic plots of protein. *J. Appl. Crystallogr.*, **24**, 946–950.
 Mengin-Lecreux,D. and van Heijenoort,J. (1990) Nucleotide sequence of the *murD* gene encoding the UDP-MurNAc-L-Ala-D-Glu synthetase of *Escherichia coli*. *Nucleic Acids Res.*, **18**, 183.
 Mengin-Lecreux,D., Parquet,C., Desviat,L.R., Plá,J., Flouret,B., Ayala,J.A. and van Heijenoort,J. (1989) Organization of the *murE–murG* region of *Escherichia coli*: identification of the *murD* gene encoding the D-glutamic-acid-adding enzyme. *J. Bacteriol.*, **171**, 6126–6134.

- Michaud,C., Parquet,C., Flouret,B., Blanot,D. and van Heijenoort,J. (1990) Revised interpretation of the sequence containing the *murE* gene encoding the UDP-*N*-acetylmuramyl-tripeptide synthetase of *Escherichia coli*. *Biochem. J.*, **269**, 277–278.
- Michelson,A.M., Dondon,J. and Grunberg-Manago,M. (1962) The action of polynucleotide phosphorylase on 5-halogenouridine-5' pyrophosphate. *Biochim. Biophys. Acta*, **55**, 529–540.
- Moy,J.-P. (1994) A 200 mm input field, 5–80 keV detector based on an X-ray image intensifier and CCD camera. *Nucl. Instrumen. Methods Phys. Res.*, **A348**, 641–644.
- Noel,J.P., Hamm,H.E. and Sigler,P.B. (1993) The 2.2 Å crystal structure of transducin- α complexed with GTP γ S. *Nature*, **366**, 654–663.
- Pai,E.F., Kabsch,W., Krengel,U., Holmes,K.C., John,J. and Wittinghofer,A. (1989) Structure of the guanine-nucleotide-binding domain of the Ha-ras oncogene product p21 in the triphosphate conformation. *Nature*, **341**, 209–214.
- Pai,E.F., Krengel,U., Petsko,G.A., Goody,R.S., Kabsch,W. and Wittinghofer,A. (1990) Refined crystal structure of the triphosphate conformation of H-ras-p21 at 1.35 Å resolution: implications for the mechanism of GTP hydrolysis. *EMBO J.*, **9**, 2351–2359.
- Parquet,C., Flouret,B., Mengin-Lecreux,D. and van Heijenoort,J. (1989) Nucleotide sequence of the *murF* gene encoding the UDP-MurNAc-pentapeptide synthetase of *Escherichia coli*. *Nucleic Acids Res.*, **17**, 5379.
- Poland,B.W. and Honzatko,R.B. (1993) Crystal structure of adenylosuccinate synthetase from *Escherichia coli*. *J. Biol. Chem.*, **268**, 25334–25342.
- Pratviel-Sosa,F., Mengin-Lecreux,D. and van Heijenoort,J. (1991) Overproduction, purification and properties of the uridine diphosphate *N*-acetylmuramoyl-L-alanine: D-glutamate ligase from *Escherichia coli*. *Eur. J. Biochem.*, **202**, 1169–1176.
- Ramachandran,G.N., Ramakrishnan,C. and Sasisekharan,V. (1963) Stereochemistry of polypeptide chain configurations. *J. Mol. Biol.*, **7**, 95–99.
- Ramakrishnan,V., Finch,J.T., Graziano,V., Lee,P.L. and Sweet,R.M. (1993) Crystal structure of globular domain of histone H5 and its implications for nucleosome binding. *Nature*, **362**, 219–223.
- Rogers,H.T., Perkins,H.R. and Ward,J.B. (1980) *Microbial Cell Walls and Membranes*. Chapman & Hall Ltd, London, UK, pp. 239–297.
- Rossmann,M.G., Liljas,A., Branden,C.I. and Banaszak,L.J. (1975) Evolutionary and structural relationships among dehydrogenases. In Boyer,P.D. (ed.), *The Enzymes*. Academic Press, New York, pp. 61–102.
- Saraste,M., Sibbald,P.R. and Wittinghofer,A. (1990) The P-loop, a common motif in ATP- and GTP-binding proteins. *Trends Biochem. Sci.*, **15**, 430–434.
- Schleifer,K.H. and Kandler,O. (1972) Peptidoglycan types of bacterial cell walls and their taxonomic implications. *Bacteriol. Rev.*, **36**, 407–477.
- Schulz,G.E. (1992) Binding of nucleotides by proteins. *Curr. Opin. Struct. Biol.*, **2**, 61–67.
- Schönbrunn,E., Sack,S., Eschenburg,S., Perrakis,A., Krekel,F., Amrhein,N. and Mandelkow,E. (1996) Crystal structure of UDP-*N*-acetylglucosamine enolpyruvyltransferase, the target of the antibiotic fosfomicin. *Structure*, **4**, 1065–1075.
- Sheldrick,G.M. (1990) Phase annealing in SHELXS-90: direct methods for larger structures. *Acta Crystallogr.*, **A46**, 467–473.
- Skarzynski,T., Mistry,A., Wonacott,A., Hutchinson,S.E., Kelly,V.A. and Duncan,K. (1996) Structure of UDP-*N*-acetylglucosamine enolpyruvyl transferase, an enzyme essential for the synthesis of bacterial peptidoglycan, complexed with substrate UDP-*N*-acetylglucosamine and the drug fosfomicin. *Structure*, **4**, 1465–1474.
- Tanner,M.E., Vaganay,S., van Heijenoort,J. and Blanot,D. (1996) Phosphinate inhibitors of the D-glutamic acid-adding enzyme of peptidoglycan biosynthesis. *J. Org. Chem.*, **61**, 1756–1760.
- Vaganay,S., Tanner,M.E., van Heijenoort,J. and Blanot,D. (1996) Study of the reaction mechanism of the D-glutamic acid-adding enzyme from *Escherichia coli*. *Microbial Drug Resistance*, **2**, 51–54.
- van Heijenoort,J. (1994) Biosynthesis of the peptidoglycan unit. In Ghuyssen,J.M. and Hakenbeck,R. (eds), *Bacterial Cell Wall*. Elsevier Science B.V., Amsterdam, pp. 39–54.
- Walker,J.E., Saraste,M., Runswick,M.J. and Gay,N.J. (1982) Distantly related sequences in the α - and β -subunits of ATP synthetase, myosin, kinases and other ATP-requiring enzymes and a common nucleotide binding fold. *EMBO J.*, **8**, 945–951.
- Wierenga,R.K., DeMaeyer,M.C.H. and Hol,W.G.J. (1985) Interaction of pyrophosphate moieties with α -helices in dinucleotide binding proteins. *Biochemistry*, **24**, 1346–1357.
- Yamaguchi,H., Kato,H., Hata,Y., Nishioka,T., Kimura,A., Oda,J. and Katsube,Y. (1993) Three-dimensional structure of the glutathione synthetase from *Escherichia coli* B at 2.0 Å resolution. *J. Mol. Biol.*, **229**, 1083–1100.
- Yamashita,M.M., Almasy,R.J., Janson,C.A., Cascio,D. and Eisenberg,D. (1989) Refined atomic model of glutamine synthetase at 3.5 Å resolution. *J. Biol. Chem.*, **264**, 17681–17690.

Received on February 26, 1997; revised on March 17, 1997